Scattering of Circularly Polarized Terahertz Waves on a Graphene Nanoantenna

Zhi-Kun Liu(刘志坤), Ya-Nan Xie(谢亚楠)**, Li Geng(耿莉), Deng-Ke Pan(潘登科), Pan Song(宋盼)

Key Laboratory of Specialty Fiber Optics and Optical Access Networks, Shanghai University, Shanghai 200072

(Received 1 September 2015)

We present a surface current method to model the graphene rectangular nanoantenna scattering in the terahertz band with Comsol. Compared with the equivalent thin slab method, the results obtained by the surface current method are more accurate and efficient. Then the electromagnetic scattering of circularly polarized terahertz waves on graphene nanoantennas is numerically analyzed by utilizing the surface current method. The dependences of the antenna resonant frequency with the circularly polarized wave on width and length are consistent with those for the linear polarized waves. These results are proved to be useful to design efficient nanoantennas in terahertz wireless communications.

PACS: 78.67.Wj, 84.40.Ba, 73.20.−r DOI: 10.1088/0256-307X/33/2/027802

Graphene, single atomic thick layer of hexagonally latticed carbon atoms, has recently attracted tremendous interest due to its unique electrical, optical, thermal, chemical and mechanical properties.[1−5] Graphene allows us to utilize the novel physics in a plethora of potential applications such as liquid crystal devices,[6] utra-high-speed transistors,[7] supercapacitors,[8] and graphene plasmonics.[9−12] One potential application of graphene is wireless communications, which cannot be achieved by using classical metallic antennas with a few micrometers due to the following drawbacks: low mobility of electrons in nanoscale metallic structures and high resonant frequencies in infrared and optical regions. However, graphene provides an adequate condition for the existence of surface plasmon polaritons (SPP),[9] which propagate along the interface between graphene and air. It has a dramatically lower frequency and higher radiation efficiency with respect to their metallic counterparts.[13]

There are two main ways to model a graphene sheet. The first technique is generally called the equivalent thin slab model (ETSM).[13,14] The graphene sheet is approximated as a three-dimensional thin slab with a small size and finite width. However, numerical computation of the electromagnetic fields requires a high computational cost in this model. The second is known as the equivalent impedance surface model (EISM).[13−15] The graphene sheet can be modelled as an equivalent impedance surface. Electromagnetic scattering problems can be numerically solved by the two-dimensional method of moments (MoM-2D). However, this model can only be used for simulation of some simple problems of graphene. For solving those drawbacks of the above models, we present the surface current method (SCM) to simulate the scattering property of graphene antennas with the finite element method (FEM) commercial software Comsol. These results are proved to be useful for designing efficient nanoantennas in terahertz wireless communications.

In this work, we present a numerical analysis of the terahertz radiation scattering on a graphene nanoantenna with rectangular geometry (Fig. 1). When the planar antenna is illuminated by linear polarized wave, the absorbing cross section of this planar structure is calculated by utilizing SCM and ETSM with Comsol. In the case of the circularly polarized terahertz waves illustrated, the absorbing cross section and the resonances of nanoantennas with different sizes are analyzed, and the electric field is also calculated in the x–y plane when using SCM.

Experiments have demonstrated that the edge effects on the graphene conductivity can be disregarded[16] in structures with lateral dimensions larger than 100 nm, and the surface conductivity of graphene nanoantennas can be computed by using the Kubo formula.[17,18] The graphene nanoantenna in this study is several micrometers. We just consider the intraband Drude contribution within the random-phase approximation for graphene surface conductivity[13]

$$\sigma_{2\mathrm{D}} = \frac{2e^2}{\pi\hbar}\frac{k_{\mathrm{B}}T}{\hbar}\ln\left[2\cosh\left[\frac{\mu_{\mathrm{c}}}{2k_{\mathrm{B}}T}\right]\right]\frac{i}{2\pi f + i\tau^{-1}}, \quad (1)$$

where τ is the relaxation time, μ_{c} is the chemical potential, and T is the temperature. Here $\tau = 10^{-13}$ s, $T = 300$ K and $\mu_{\mathrm{c}} = 0$ eV. The intraband contribution in Eq. (1) dominates over the interband one below 5 THz,[19] thus it is a reasonable approximation in our studied frequencies here.

When the object is a three-dimensional structure, the absorbing cross section related with volume V can be defined as follows:

$$\sigma_{\mathrm{abs}} = \iiint Q dV / I_0, \quad (2)$$

**Corresponding author. Email: yxie@shu.edu.cn

© 2016 Chinese Physical Society and IOP Publishing Ltd

where I_0 is the incident intensity and Q is the power loss density,

$$Q = \mathrm{Re}(\boldsymbol{J}^* \cdot \boldsymbol{E})/2. \tag{3}$$

Tensor of graphene conductivity within ETSM is defined as[20,21]

$$\sigma_{3D} = \begin{pmatrix} \sigma_{2D}/h_0 & 0 & 0 \\ 0 & \sigma_{2D}/h_0 & 0 \\ 0 & 0 & 0 \end{pmatrix}, \tag{4}$$

where h_0 is the equivalent thickness of slab.

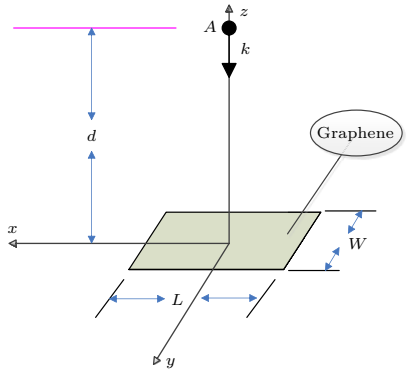

Fig. 1. Sketch of the graphene nanoantenna.

When the object is a two-dimensional structure, in SCM, electric surface current $\boldsymbol{J}_s$ is given by the product of surface conductivity σ_{2D} and tangential component $\boldsymbol{E}_t$ of electric field by $\boldsymbol{J}_s = \sigma_{2D}\boldsymbol{E}_t|_{z=0}$ on the graphene surface. The electromagnetic field can be calculated using boundary conditions at the graphene interface,

$$\boldsymbol{n} \cdot [\boldsymbol{B}|_{z=+0} - \boldsymbol{B}|_{z=-0}] = 0, \tag{5}$$

$$\boldsymbol{n} \times [\boldsymbol{H}|_{z=+0} - \boldsymbol{H}|_{z=-0}] = J_s. \tag{6}$$

We have

$$\boldsymbol{J}^* \cdot \boldsymbol{E} = J_x^* E_x + J_y^* E_y = \sigma_{2D}^* |E_x|^2 + \sigma_{2D}^* |E_y|^2. \tag{7}$$

Then we can obtain

$$\sigma_{\mathrm{abs}} = \frac{\iint \mathrm{Re}[\sigma_{2D}^* |E_x|^2 + \sigma_{2D}^* |E_y|^2] dxdy}{2I_0}, \tag{8}$$

where σ_{2D}^* is the conjugation of the graphene surface conductivity σ_{2D}. We can simulate the graphene nanoantennas by using ETSM and SCM according to Eqs. (2) and (8), respectively.

Figure 2 shows a comparison between the results of SCM and ETSM. The incidence direction of the linear polarized wave is perpendicular to the plane of the graphene antenna, and the polarized direction of electric field $\boldsymbol{E}$ parallel to the length L of the antenna (Fig. 1). The antenna is placed in a vacuum. The rectangular geometry is described by the length $L = 4\,\mu\mathrm{m}$ and the width $W = 1\mu\mathrm{m}$. The equivalent thickness h_0 of the graphene sheet is zero by using SCM. The thicknesses h_0 are 20 nm and 50 nm in ETSM. In Fig. 2, we can observe that the results of ETSM approach SCM when the thickness h_0 is reduced. Therefore, SCM is more accurate[13] than ETSM. Since we need an extremely finer mesh for higher relation L/h_0, the computational cost of ETSM is increased for smaller h_0. However, compared with ETSM, SCM presents much lower computational cost. The time of the simulation with ETSM is more than 2.5 h, while SCM is less than 4 min. Thus SCM is more efficient than ETSM. The reason is that SCM is a 2D model method, while ETSM is a 3D method. The authors of Refs. [13,14] mainly used MoM-2D to simulate the graphene sheet, while our study mostly utilizes the 2D Comsol method (SCM). Comsol uses a finite element analysis, which is applied in various engineering and physics topics, especially coupled phenomena or multiphysics. Thus Comsol can solve more complicated graphene problems by using SCM than MoM-2D.

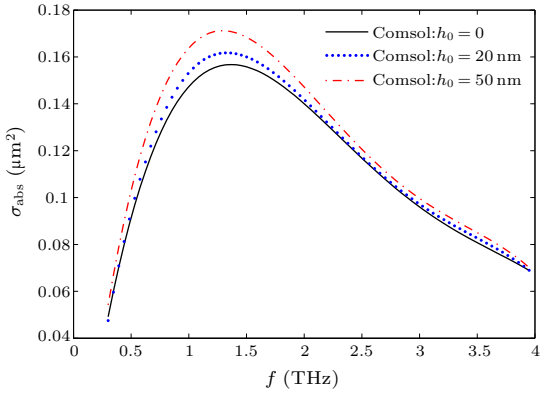

Fig. 2. Comparison of absorbing cross section of the rectangular graphene nanoantenna simulated by SCM ($h_0 = 0$) and ETSM ($h_0 = 20\,\mathrm{nm}$ and $h_0 = 50\,\mathrm{nm}$).

When a left-handed circularly polarized wave illuminates in the direction perpendicular to the plane of the antennas (shown in Fig. 1), the electric field components can be expressed as

$$E_x(t) = E_0 e^{i(\omega t - kz + kd)}, \tag{9}$$

$$E_y(t) = E_0 e^{i[(\omega t - kz + kd) + \pi/2]}. \tag{10}$$

Thus the electric field vector can be written as

$$\boldsymbol{E}(t) = E_x(t)\hat{x} + E_y(t)\hat{y}. \tag{11}$$

When the time t is zero at coordinates A (0, 0, $d = 6\,\mu\mathrm{m}$) shown in Fig. 1, we can obtain $E_x = E_0$ and $E_y = iE_0$ in terms of Eqs. (9) and (10).

In the following the dependence of the resonant frequency on width is analyzed by utilizing SCM. The value of the graphene antenna length L is $4\,\mu\mathrm{m}$. Figure 3 presents parametric analysis of the absorbing cross section σ_{abs} for different values of width W. The resonances of the antenna in Fig. 3 are 1.82 THz, 1.77 THz

and 1.44 THz corresponding to $W = 3\,\mu$m, $2\,\mu$m and $1\,\mu$m, respectively. At resonances, the maximum values of the absorption cross section are $0.30\,\mu\text{m}^2$, $0.18\,\mu\text{m}^2$ and $0.09\,\mu\text{m}^2$ for $W = 3\,\mu$m, $2\,\mu$m and $1\,\mu$m, respectively. Therefore, the resonant frequency and the absorbing cross section shift toward lower numerical values for smaller width. This is the same as that with the linear polarized wave.[13,14]

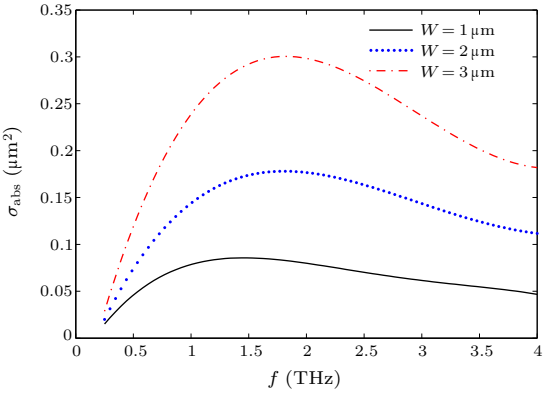

Fig. 3. Absorbing cross section of the graphene antenna for different widths $W = 3\,\mu$m, $2\,\mu$m and $1\,\mu$m in the case of circularly polarized wave illuminated.

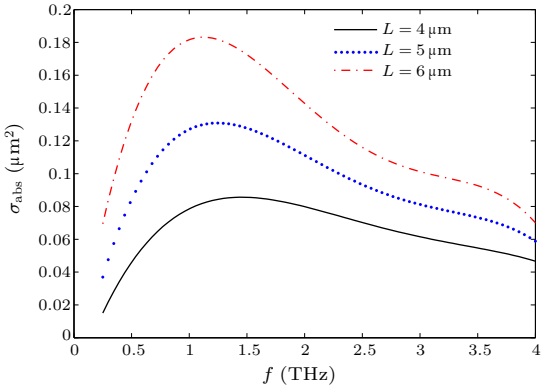

Fig. 4. Absorbing cross section of the graphene antenna for different lengths $L = 6\,\mu$m, $5\,\mu$m and $4\,\mu$m in the case of circularly polarized wave illuminated.

The dependence of the resonant frequency on the length is also analyzed. Figure 4 shows the relation of the absorbing cross section σ_{abs} and the frequency for different lengths L. When the width is set to be $1\,\mu$m, the resonances appear at 1.10 THz, 1.25 THz and 1.44 THz for $L = 6\,\mu$m, $5\,\mu$m and $4\,\mu$m, respectively. At resonances, the maximum values of the absorption cross section are $0.18\,\mu\text{m}^2$, $0.13\,\mu\text{m}^2$ and $0.09\,\mu\text{m}^2$ corresponding to $L = 6\,\mu$m, $5\,\mu$m and $4\,\mu$m, respectively. The resonance shifts towards higher frequencies for shorter antennas, and the shorter antennas possess the smaller values of absorbing cross section σ_{abs}. Therefore, the dependence of the antenna resonant frequency with the circularly polarized wave on width and length is consistent with that for the linear polarized wave.

When a left-handed circularly polarized terahertz wave transmits from point A to the graphene surface, E_x, E_y in Eqs. (9) and (10), and their phase-difference $\Delta\varphi$ is calculated in x–y plane. The parameters are $f = 1.3$ THz, $d = 6\,\mu$m, $L = 4\,\mu$m, $W = 1\,\mu$m and $E_0 = 1$. The phase differences $\Delta\varphi$ of points $(0, 0, 0)$ and $(1.5, 0.3, 0)$ on the graphene surface are not 90° listed in Table 1, which indicate that the electromagnetic wave is no longer a circularly polarized terahertz wave. However, the electromagnetic wave is still a circularly polarized terahertz wave on the point $(6, 6, 0)$ out of graphene due to $\Delta\varphi = 90°$.

Table 1. The values of E_x, E_y and $\Delta\varphi$ on different points.

	E_x	E_y	$\Delta\varphi$
$(0, 0, 0)$	$15.07+2.00i$	$-2.12+3.23i$	115.78°
$(1.5, 0.3, 0)$	$9.75+2.59i$	$-1.01+2.89i$	94.37°
$(6, 6, 0)$	$19.17-3.19i$	$3.18+19.15i$	90.02°

Finally, we verify whether the values simulated by Comsol are convergent when $d = 6\,\mu$m, $L = 4\,\mu$m and $W = 1\,\mu$m. The absorbing cross section for $d = 6\,\mu$m, $30\,\mu$m and $50\,\mu$m is shown in Figs. 5(a)–5(c) by utilizing SCM. For comparison, putting Figs. 5(a)–5(c) in the same picture is shown in Fig. 5(d). From Fig. 5(d), we can see that the absorbing cross section has no relations with d and the resonant frequency is still 1.48 THz. At resonances, the maximum value of the absorbing cross section is $0.86\,\mu\text{m}^2$. Thus the results are convergent when $d = 6\mu$m.

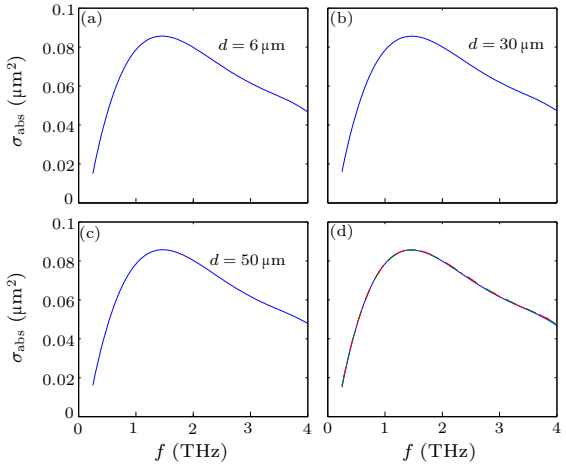

Fig. 5. The absorbing cross section of the graphene antenna for different d: (a) $d = 6\,\mu$m, (b) $d = 30\,\mu$m and (c) $d = 50\,\mu$m. For comparison, putting (a)–(c) in (d).

In conclusion, we present SCM to model scattering properties of a graphene rectangular nanoantenna in terahertz band with Comsol. The results obtained by SCM are more accurate and efficient than ETSM. Then the electromagnetic scattering of circularly polarized terahertz waves on graphene nanoantennas is numerically analyzed by utilizing SCM. The results show that the dependence of the antenna resonant frequency and absorbing cross section with the cir-

cularly polarized wave on antenna's size is consistent with that for the linear polarized wave. In addition, when a left-handed circularly polarized terahertz wave is illuminated on the graphene antenna, the electromagnetic wave is no longer a circularly polarized terahertz wave based on the value of phase difference $\Delta\varphi$ between the x-component and y-component of electric field. All the results presented in this work may be useful to simulate and design the graphene nanoantennas for applications in wireless communications.

We thank Yan Wang for help with Comsol simulations and for useful discussions, and Guangli Yang for great support. We would also like to thank Hua Gao for his valuable comments that are helpful for improvement of this work.

References

[1] Geim A K and Novoselov K S 2007 *Nat. Mater.* **6** 183
[2] Novoselov K S, Geim A K, Morozov S V, Jiang D, Katsnelson M I, Grigorieva I V, Dubonos S V and Firsov A A 2005 *Nature* **438** 197
[3] Huang Z X, Wang L Y, Bai S Y and Tang Z A 2015 *Chin. Phys. Lett.* **32** 086801
[4] Blake P, Hill E W, Castro N A H, Novoselov K S, Jiang D, Yang R, Booth T J and Geim A K 2007 *Appl. Phys. Lett.* **91** 063124
[5] Zhang W X, Liu Y X, Tian H, Xu J W and Feng L 2015 *Chin. Phys. B* **24** 076104
[6] Blake P, Brimicombe P D, Nair R R, Booth T J, Jiang D, Schedin F, Ponomarenko L A, Morozov S V, Gleeson H F, Hill E W, Geim A K and Novoselov K S 2008 *Nano Lett.* **8** 1704
[7] Schwierz F 2010 *Nat. Nanotechnol.* **5** 487
[8] Sui P F, Zhao Y C, Dai Z H and Wang W T 2013 *Chin. Phys. Lett.* **30** 0107306
[9] Jablan M, Buljan H and Soljačić M 2009 *Phys. Rev.* B **80** 245435
[10] Chen T and Lu X H 2015 *Chin. Phys. Lett.* **32** 024204
[11] Fei Z, Rodin A S, Gannett W, Dai S, Regan W, Wagner M, Liu M K, Mcleod A S, Dominguez G, Thiemens M, Castro N A H, Keilmann F, Zettl A, Hillenbrand R, Fogler M M and Basov D N 2013 *Nat. Nanotechnol.* **8** 821
[12] Garciía de Abajo F J 2014 *ACS Photon.* **1** 135
[13] Llatser I, Kremers C, Cabellos-Aparicio A, Jornet J M, Alarcon E and Chigrin D N 2012 *Photon. Nanostruct. Fundam. Appl.* **10** 353
[14] Costa K Q, Dmitriev V, Nascimento C M and Silvano G L 2013 *International Microwave and Optoelectronics Conference* (Rio de Janeiro Brazil, 4–7 August 2013) p 1
[15] Llatser I, Kremers C, Cabellos-Aparicio A, Jornet J M, Alarcon E and Chigrin D N 2011 *The Fourth International Workshop on Theoretical and Computational Nanophotonics* (Bad Honnef Germany, 26–28 October 2011) p 144
[16] Han M Y, Özyilmaz B, Zhang Y B and Kim P 2007 *Phys. Rev. Lett.* **98** 206805
[17] Falkovsky L A and Pershoguba S S 2007 *Phys. Rev.* B **76** 153410
[18] Hanson G W 2008 *IEEE Trans. Antennas Propag.* **56** 747
[19] Mikhailov S A 2007 *Europhys. Lett.* **79** 27002
[20] Vakil A and Engheta N 2011 *Science* **332** 1291
[21] Koppens F H L, Chang D E and García de Abajo F J 2011 *Nano Lett.* **11** 3370